Vol. 38, No. 3 (2016) 402-411

Tribology in Industry

www.tribology.fink.rs

RESEARCH

Wear Resistance of Nano Alumina Containing SiO_2-B_2O_3-Na_2O Glass-Ceramic on Steel Substrate

A. Faeghinia[a], A. Zamanian[a]

[a] *Ceramic division, materials and energy research center, Tehran, Iran.*

Keywords:

Nano alumina
Slip
Enamel
Coating

Corresponding author:

Aida Faeghinia
Ceramic division, materials and energy research center,
Tehran, Iran.
E-mail: aida.faeghinia@gmail.com

A B S T R A C T

The experimental study has been carried out to investigate the tribological properties of nano Alumina reinforced glass-ceramic enamel. The mixtures of (5, 10, 15 wt.%) nano alumina and glass powders have been air sprayed on stainless steel substrate.. The thixotropy, wetting angle and surface tension of used slurry were increased inherently by 15-wt.% nano alumina. By heat treating at 870-640-525 ºC, the homogeneous crystalline sodium silicate phase beside nano alumina was obtained in glass –ceramic coat. According to the EDAX results, the precipitated reduced Sb and Mo particles at the interface of enamel and steel caused to reasonable adherence of coat and steel. The dry sliding wear tests were carried out using pin on disk method. Results revealed the 0.01 mg wear rate by 30N load at 100 m for nano alumina bearing coats. The wear resistance increased by a factor of 10. According to SEM micrographs, the sliding load transfer by nano alumina particles occurred.

1. INTRODUCTION

It is known that under industrial conditions, the wetting of enamel slip on substrate is important, which after its preparation, the processes of frites drying, can be achieved appropriately. On applying the enamel suspension, the covering capacity depends on slips surface tension, viscosity, flow ability, etc. These needs additional improvement by adding electrolytes and changing the firing process (heating rate, heating atmosphere, ...) [1]. It was found that the processing window for successful deposition of glass coatings at high rate is narrow.

Moreover, it was shown that, the size of filler components in the nano-scale have effects on the mechanical properties of enamel. Positively affect brittle-fracture properties and also there is the possibility of using applications in dental implantology [2] The multiple regression models was predicted the wear rate with higher accuracy for different quartz addition, and thermal treatment conditions in silica-glass composite coatings as well [3].

The plan to reduce coats wear is to first alteration the material of the component to those that have higher hardness, higher strength and long survivals. However, the decision is not

always possible because of the following reasons: (i) it is not economical in many conditions and (ii) the concerned component is so complex in shape and design that exactly it is not practicable to change the material. The other strategy will be to change the surface so that it has higher hardness. This can be done through surface diffusion of materials or alternately by applying a coating on the surface [3]. The coating can be of a polymer or of a glass–ceramic. The benefit of a glass–ceramic coating is that it is chemically inert, can withstand high temperature (up to ~1000 °C) and has superior mechanical properties compared to polymer and other non-oxide coatings, viz. paints, metals, rubbers, etc. [4]. A glass ceramic coating often allows more flexibility in design as it can with stand much wider mechanical and thermal cruelties.

This paper describes the preparation, application, of a new enamel coating, which applied directly on steel panels. The effects of nano-alumina addition on rheological and wear properties of obtained enamel and coat were discussed.

2. MATERIALS AND METHOD

Frit composition denoted by G1 was selected from references [5] .The frit was prepared from reagent grade chemicals: SiO_2, Al_2O_3, $BaCO_3.10H_2O$, $CaCO_3$, Na_2CO_3, ZnO, $H_2P_2O_5$, and CaF_2. The chemical composition of the frit was listed in Table 1.

Table 1. The chemical composition of frit.

wt.%	SiO_2	Al_2O_3	ZnO	B_2O_3	CaO	P_2O_5	Na_2O
1	40	11	8	20	2	2	17

The batch was regularly blended in ball mill and was melted in Alumina crucible in resistance furnace at 1250 ˚C, the batch was hold at this temperature for 2 h in order to reach homogeneous, bubble-free melts. Then a stream of the smelted and refined molten batch is drawn from the alumina crucible and quenched into water to produce a coarse granular frit .The frits were milled using a ball mill with alumina ball as the grinding media for 24 h. and screened with a mesh size of 200 mesh, stored in an oven at 100 ˚C to remove the moisture. The powder size distribution exhibited a Gaussian distribution in particle size with a cumulative weight percent average of ≈5 μm. The powder size distributions determined by laser diffraction using a Malvern Master Sizer 2000 as were shown in Fig. 1. The frits were further processed by mixing with certain mill-additive (sodium alginate) to make thick slurry called "slip" to make uniform and thin coating on the clean metal parts by spraying technique. Kaolinite, borax and water, Sb_2O_3, MoO_3 were added to form a batch of enamel slip (Table 2).

Table 2. The wt.% of milling additives.

Additive	Frit	Clay	Water	Sb_2O_3	MoO_3	Nano Al_2O_3
wt.%	100	3	60	1.3	2.9	5-10-15

In this step the excess amount of nano alumina particles were added to the G1 samples by 5, 10, 15 wt.% which the samples denoted by GA5, GA10, GA15 respectively.

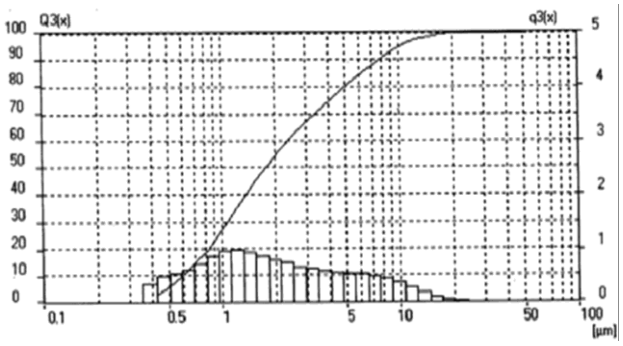

Fig 1. The particle size distribution of G2.

The mass ratio of solid to water in all mixtures was 78/22. Aqueous frit suspensions at 70 vol.% solid loading were prepared using Sodium Alginate (1.2 wt.% based on solid weight). Each slip was prepared by solving of the dispersant in water and subsequent pouring of mixed powders in the dissolved dispersant. The resultant slurry was stirred for 1 h and then ultrasonically agitated for 3 min.

The rheological properties of coating material slips are very important in point view of proper application of the coating. The specific gravity of the enameling slip was measured using an electronic weighing balance and was controlled between (1.7-1.8 g/cm^3) by adjusting the water content. Subsequently, the slip was aged for 24 hours before enameling to improve its fluidity.

The rheological properties were studied using a Reostat-2 devise with coaxial cylinders. The

ultimate dynamic shear stress τ was found by extrapolating the linear region of the flow curve (dependence of the deformation rate on the shear stress) to the abscissa and measuring a segment cut from it, the viscosity ɳ was found by determining the cotangent of the angle of slope of this region to the abscissa. To gather data about the slip droplets, freeze image analysis was employed to measure the contact angle and surface tension. Therefore, a standstill digital camera (Canon, Japan) complete was used to assist in the image capture during the detachment process [6].

2.1 Substrate preparation

Steels samples (316 alloy) were obtained by cutting annealed 1.5 in. diameter. The bars stock in to disks of 5 mm thickness, which were then cut into quarter-disk coupons for testing. The steel substrates were degreased and grit blasted to give a surface with a R_a value of 2 mm immediately before spraying**.**

2.2 Application of enamel slip

The Air Spray coatings were manufactured using nozzle with 0.5 mm internal diameter, using an argon. Slips were injected externally of the nozzle using an inject or of 0.5 mm in internal diameter, Particles were carried into the jet by argon gas having a flow rate of 7 SLM and setting the powder flow rate in 30 g/ min. The standoff distance was 100 mm. The green deposit was slowly dried in air, followed by heating in an air oven at ~120 °C for complete drying. The weight of the deposit (0.2 g) was measured by weighing the plates before and after the deposition. Subsequently, the coatings were examined visually for surface quality.

2.3 Firing of the enamels

The achieved enamels were heat treated according to the DTA results at almost melting temperature of the obtained frit for 5-10 minute (dependent on composition) and then the nucleation and growth temperature were chosen for further crystallization of the enamel (at 525 ºC/30 min and 640 ºC/30 min.). Crystalline phase identification was performed on coated samples, using X-ray diffraction (Philips Power Diffracto meter 1710) with Ni- filtered Cu- K α radiation and the relevant JCPDS cards (Joint Committee on Powder Diffraction, 1972).

2.4 Wear test

Pin-on-disk the most widely used wear test processes, followed by pin-on-flat other applications of pin-on-disc include material wear and friction properties at elevated temperatures and in controlled atmospheres.

Wear tests were performed in accord with the ASTM:G99-95a for wear testing with a pin-disk. The counter specimen was a pin mad from ball bring steel 52100 (micro hardness 66 Rockwell C), a load at frictional contact F = 30 N, linear sliding speed v = 0.5 m/s, total sliding length s = 200 m, friction radius r_t = 13 mm. The wear rate expressed in (mg/m) is calculated as follows:

$$W_R = \frac{\Delta w}{S}$$

where: W_R: wear rate, Δw: weight loss in (mg), s sliding distance in (m). A wear coefficient is often used to categories resistance to contact wear. All of the tests were conducted at ambient atmospheric condition at room temperature 25 ˚C and 23 % humidity. Lubrication is not applied to avoid the complication of thermochemical effects Scanning electron microscopy (SEM: model JEOL JXA-840) was used in order to observe the microstructure and EDX analysis. Samples were mounted onto the sample holder, coated with gold, and then studied with SEM.

3. RESULTS

Figure 2a show the characteristic flow curves for the systems under investigation, obtained with the help of a" Rheotest-2" instrument. One curve (1a) shows the process of disintegration of the structure at constant increase in the rate of sharing, and the other curve shows the reverse process of structure formation under subsequent decrease in j (1b). The area of the hysteresis loop thus formed is different for different slips and is a function of the thixotropic nature of the system [4,5]. The larger the loop area, the stronger is the thixotropic tendency. The flow curves of the slips under investigation and a comparison of the shape and area of the hysteresis loops showed that the introduction of

nano-alumina in the slip composition enabled one to control its thixotropic nature.

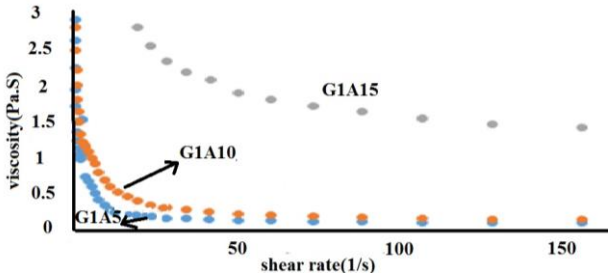

Fig. 2a. Flow curves of the enamel slip (a) G1A5 (b) G1A10 (c) G1A15.

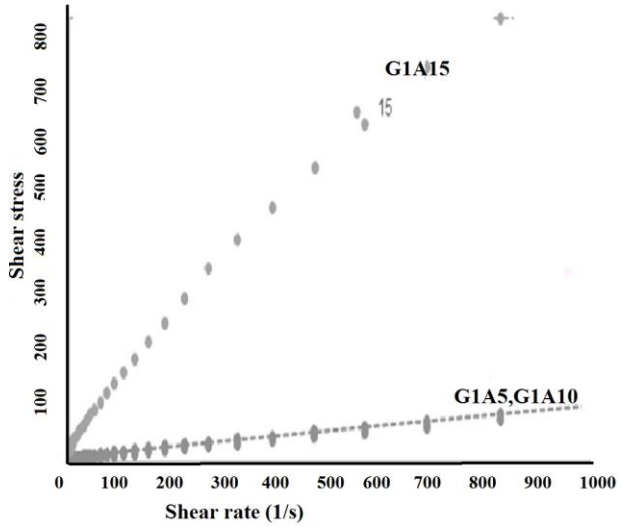

Fig. 2b. Shear stress vs. shear rate of enamel slip (a) G1A5 (b) G1A10 (c) G1A15.

Figure 2b shows viscosity vs. shear rate of enamels. As indicated, the dilatant condition was reduced in curve GA15. The effect of the alumina is shown by comparing the larger apparent viscosity of curve GA15 to GA10. An explanation of this phenomenon is based on the theory that due to the formation of an insoluble complex between the flocculating alumina ions and the solution silicate ions [7]. It is clear from the Figs. 2 that the alumina has a significant effect on η and τ.: Dilution of the slip produces an intense reduction in these values. A similar dependence has been established in a study of the rheological properties of aqueous suspensions of quartz sand with an addition of clay [6]. The results show that by increasing the stress shear rate the viscosity of the slips decreased.

3.1Wetting angle:

Surface tension determines the tendency of a liquid surface to resist external force. In this case ,the wetting angle of the alumina bearing slip (Fig. 3) was increased from 44 to 69 º as the concentration of nano- alumina increased from 5 to 15 wt.%.

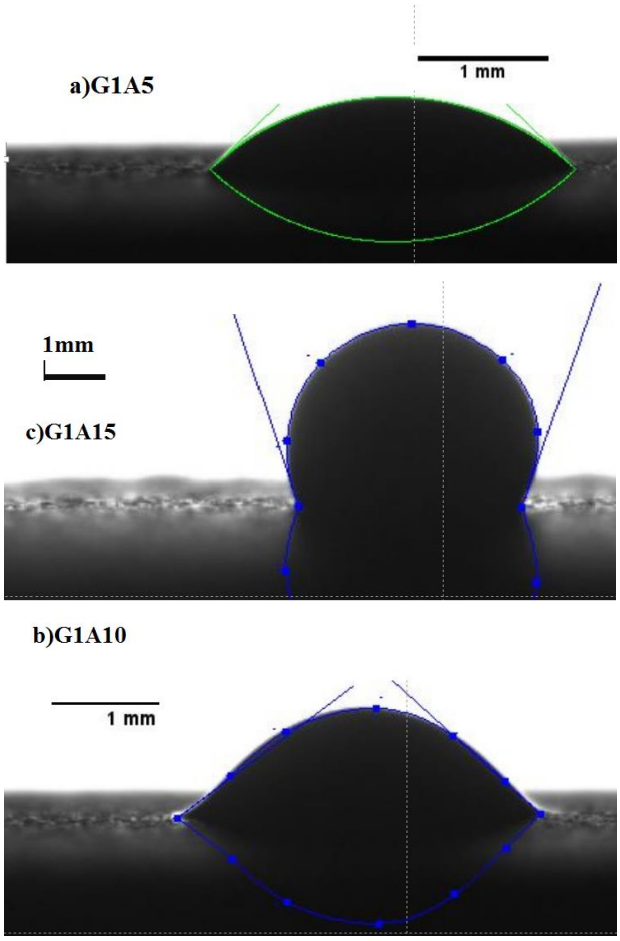

Fig. 3. The images of wettability of steel by alumina bearing system (a) G1A5 (b) G1A10 (c) G1A15.

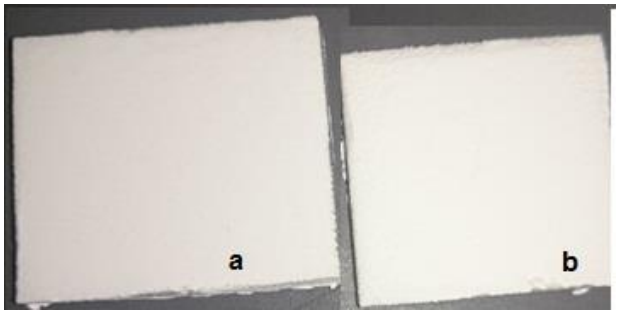

Fig. 4. (a) corresponds to the green enamel on the steel surface G1A5 (b) G1A15.

These findings are in agreement with other reported work elsewhere [7]. The main reason behind these findings can be attributed to the solid particles properties. Hydrophilic particles, whether colloidal or larger, could increases the equilibrium surface tension of an aqueous slurry e.g. from the surface tension of water, for ex.

From 72 mN/m, to 82 mN/m. As nano- alumina particles are hydrophilic and almost dissolve in water they can not produce a stable suspension for long time. It can be seen that although the alginate electrolyte was used in slurry, the surface tension of slurry was high. However, the appearance of the applied wet enamel on the steel surface was reasonable (Figs. 4a and 4b).

3.2 DTA results

Figure 5a presents the DTA results of the G1 frit and G1A5dried slurry powder. The glass melting range was get board compared to the frit curve alone; indicating that, the nano alumina particles lowered the mobility of glass particles, also the crystallization peak intensity of glass was board. It was reported before that [8], the nano alumina addition could promote the crystallization, but lowered the crystallization rate; this occurrences can be seen in the present system as well. However the coat was heat traded at 870 ºC for 5 minute followed by 525 and 640 ºC heating for 30 min. During the heat treating by 10 ºC/min rate, due to the mentioned high surface tension of enamel, the frit grains did combine with one another and form large spherical drops on the substrate.

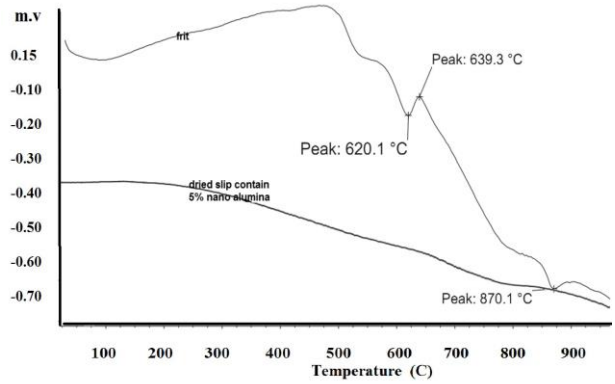

Fig. 5a. DTA results of frit and dried nano alumina containing slurry G1A5 (5b) the appearance of the G1A15 sample.

The shape and size of the near spherical mass were dependent on the firing rate, alumina amount and temperature. However, for suppressing the high surface tension of resulted melt at firing temperature, the heating rate was increased up to 300 ºC/min that minimized the spherical appearance of the alumina containing melt (or enamel) at firing temperature. The appearance of the enamels was according to Fig. 5b.

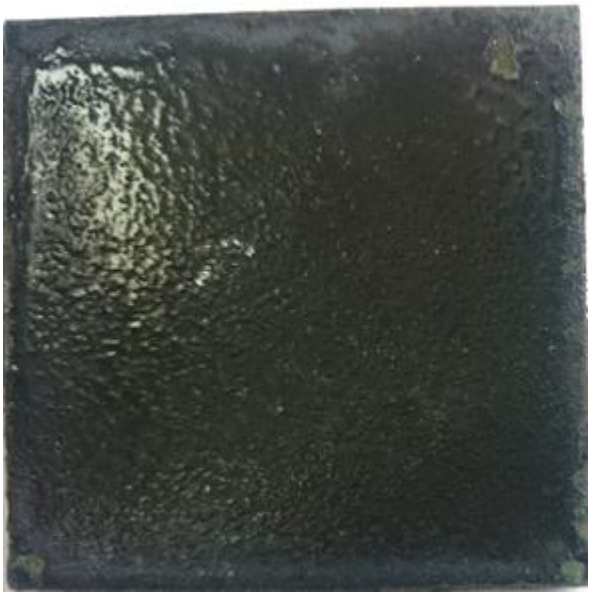

Fig. 5b. The appearance of the G1A15 sample.

However, residual porosity can be seen in all enamels appearances, by small black dots. It is formed by entrapped air during enamel fusing. It is commonly seen in dental restorations and is minimized by using vacuum during the firing cycle of the veneering enamel in dental restorations. In this study, the vacuum was not used in firing. Consequently, it can be said that , using nano alumina in enamels slip, caused to some restriction in slip applying and sintering as well.

3.3Phase evaluation of G1

The base coating (without nano alumina) was heat treated by (10 ºC/min) isothermally at 870 ºC (5 min), 525 ºC (30 min) and 639 ºC (30 min.) respectively. The typical XRD pattern of heat treated sample coating material is shown in Fig. 6.

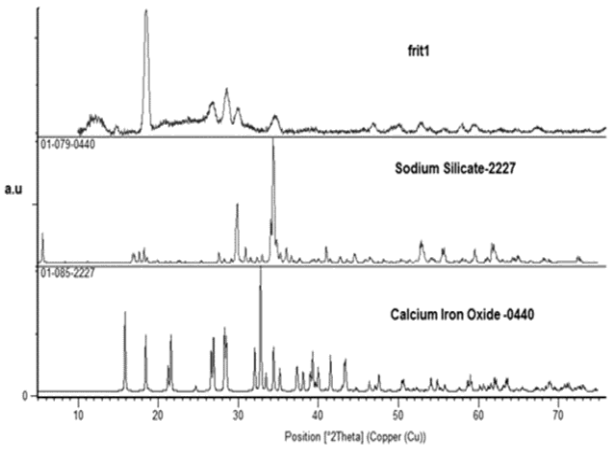

Fig. 6. The XRD pattern of G1 heat treated at three steps -870-525-640 ºC, sodium silicate was detected.

Obviously, the sodium silicate phase is the major crystalline phase in glass-ceramic. In concrete industry, it was reported that the application of sodium silicate to the steel surface produced strength bond with concrete, which increases the wear resistance of concrete [9]. Therefore, it can be said that, sodium silicate formation help the bonding of studied glass and the steel substrate with accepted wear resistance in our case as well.

3.4Microstructural evaluation of interface

Thorough examination of the cross-sectional microstructures the typical data from EDS examination of the polished cross-section of the glass-ceramic (heat treated G1) coat are presented in Figs. 7-8.

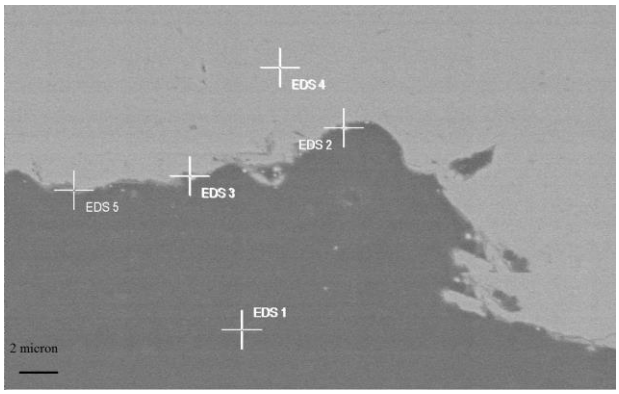

Fig. 7a. The interface of G1- alloy, consider the light points position.

The galvanic corrosion of the base iron by glassy phase at selective random points, caused to the increased roughness of interface [10]. This roughness could improve the mechanical coupling (Fig. 7a).

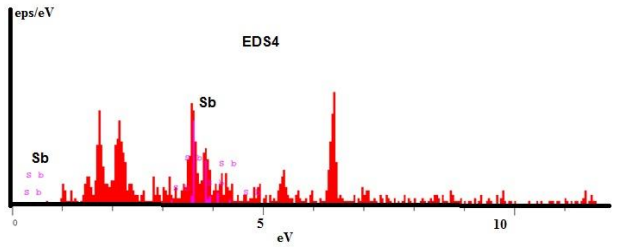

Fig. 7b. The EDS results of white marked area denoted eds4 (in Fig. 7a, G1).

It was reported that the molybdenum oxide in the glass composition helps the adhesion of enamel to steel substrate [11]. Beside the molybdenum oxide, the antimony oxide assists the Fe precipitation at the enamel –steel interface [12]. The white phases in Fig. 8a evidence the migration of listed above oxides to the boundary layer (see also the EDS of points in Fig. 8b) these points are nanometer and evidently were trapped in the anchors of interface.

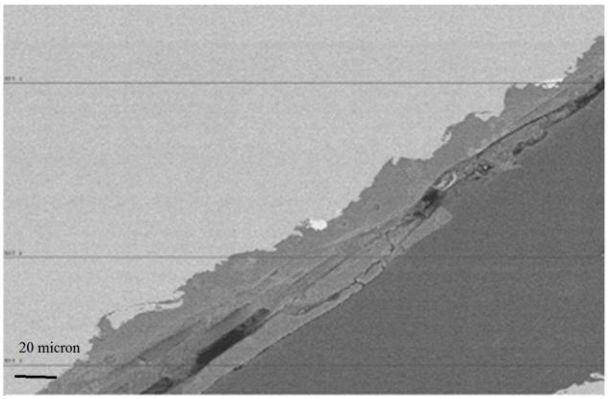

Fig. 8a. The interface of G 1A5 and substrate (with ×1000 magnification) the large white phase at the interface is observed.

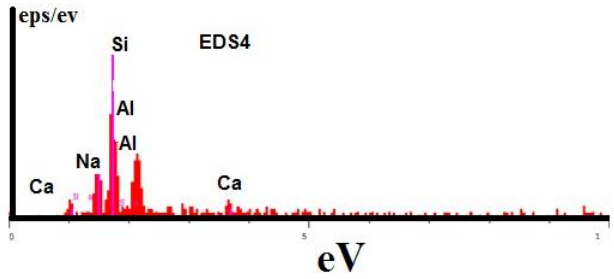

Fig. 8b. The dark gray phase below the interface of steel and G1, Si, Al, Na were detected.

It is well known that, by heating the molybdenum and antimony oxide in a non-oxidizing atmosphere the reduction of this oxide by reaction with the iron base take place and thereby they diffuse to the surface of the base. So the FeO is formed during firing, dissolve in vitreous enamels, acting as a mutual bonding agent.

3.5 Wear resistance

Figure 9 shows the wear test results of base substrate, glass (G1), glass-ceramic and composites (5 %, 10 %, 15 % nano alumina). The weight losses of samples vs. sliding distance define the wear rate and friction coefficient. According to results, while the base substrate (without coating) shows 0.2 mg weight loss in 50 m. the maximum weight loss of glass is 37 mg in 50 m. In comparison, a drastic reduction in wear loss is observed by adding 15 wt.% nano –

alumina as complementary reinforcements to make hybrid composite, where weight loss is 0.01 milligram in 100 m. As measured in G1A15. It can be said that the wear resistance of coated sample was improved up to 10 times compared to the uncoated sample.

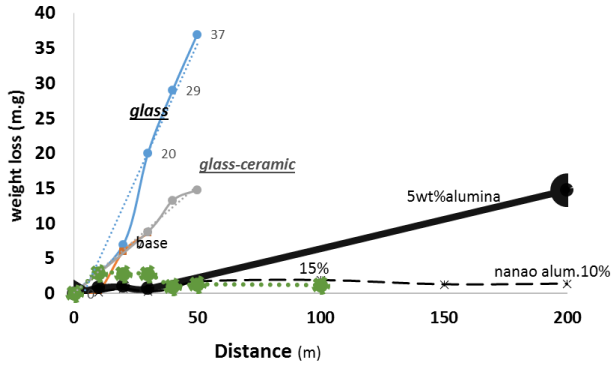

Fig. 9. The weight loss vs. distance of samples.

The wear resistance reaches a plateau at low distances (50m), which corresponds to the changeover from a glass matrix to an alumina matrix. The sliding better resistance of nano alumina bearing coating (at 30 N normal load and 0.5m/s sliding velocity), compared to G1 may be mainly due to its higher hardness associated with the larger amount of total alumina with homogeneous sodium silicate phase in glass-ceramic system.

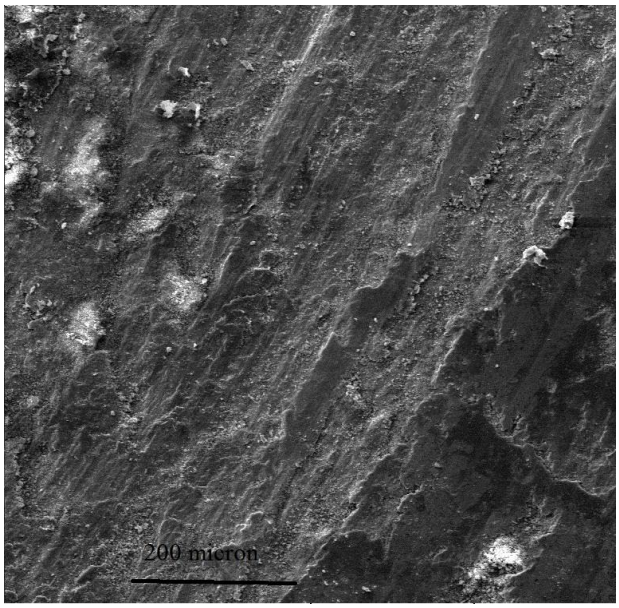

Fig. 10. The smooth surface on the worn surface of G1A15 samples.

The increase in hardness is due to reason that under the action of a compressive force and adhesive bonding, the glass/Al_2O_3 composite matrix will be pressed together and offers the resistance. Because of this resistance, the interface can transfer load easily to interfacial bonding between the matrix and fillers. The presence of adhesive bonding, which enables load transfer from the matrix to the alumina, is the main factor influencing the increase in mechanical properties [13]. Figure 10 shows the smooth surface on the worn surface of G1A15 samples which again concedes the load transfer reinforcing mechanism.

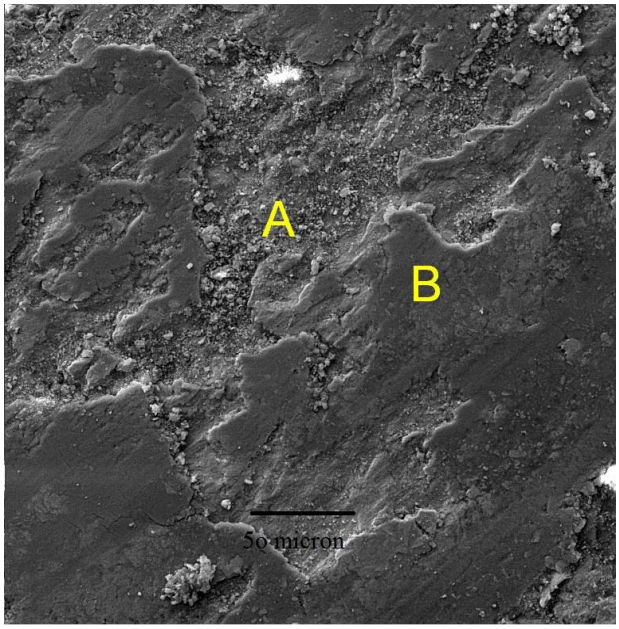

Fig. 11. (A) the fragmented and (B) smoothed surface on the worn surface of G1A15.

In addition, some parallel ploughs and grooves along the applied load were observed which could be pointed to the abrasive wear mechanism. The smooth and fragmented points analysis were compared in Tables 3 and 4, which did not detect any reasonable difference between two areas.

Table 3. Element analysis of point b.

	wt.%
Oxygen	31.02
Sodium	3.96
Aluminum	3.30
Silicon	5.41
Calcium	0.47
Chromium	5.11
Iron	40.88
Zinc	1.04
Molybdenum	0.70

Table 4. Element analysis of point a.

	wt.%
Oxygen	33.37
Sodium	2.97
Aluminum	2.77
Silicon	4.91
Calcium	0.48
Chromium	4.93
Iron	47.77
Zinc	1.70

In the case of G1A5 in Fig. 12, some scale-like structure in contact with the pin was observed that could be derived from the shear stress. This effect in G1A15 was observed less.

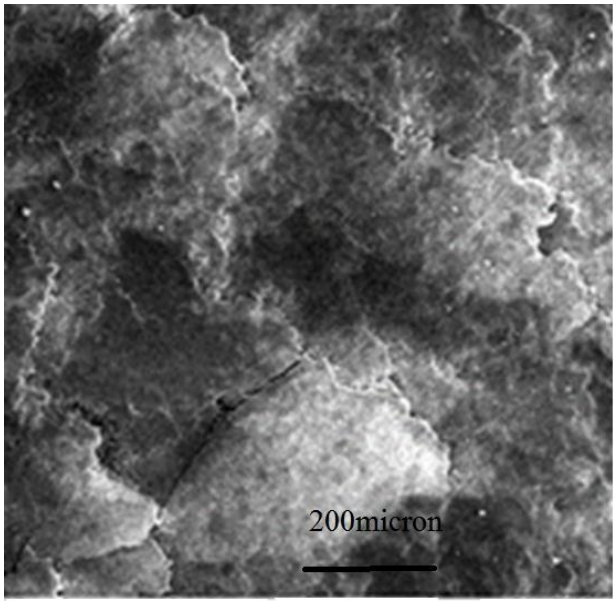

Fig. 12. Some scale-like structure in G1A5.

Some cracks around the pin effect and scaling pits exist in G1A5 and G1A10. (Figs. 13a and 13b). The wear process of these coating can be resulted from the brittle scale delamination. It should be mentioned that due to the low amount of reinforcing agent, (in G1A5.G1A10) the inhomogeneity of microstructure and consequently the inadequate hardness of microstructure caused to the disturbed cracks around the sliding track.

It is well known that, [14] because of low TEC (Thermal Expansion Coefficient), BAS (Boro alumino silicate) systems have compatibility with steels which made them appropriate for sealing application.

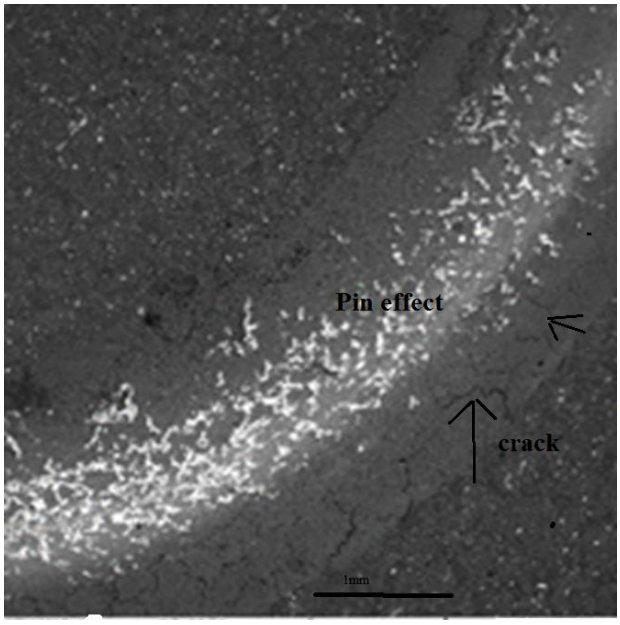

Fig. 13a. Cracks around the pin effect and scaling pits exist in G1A5.

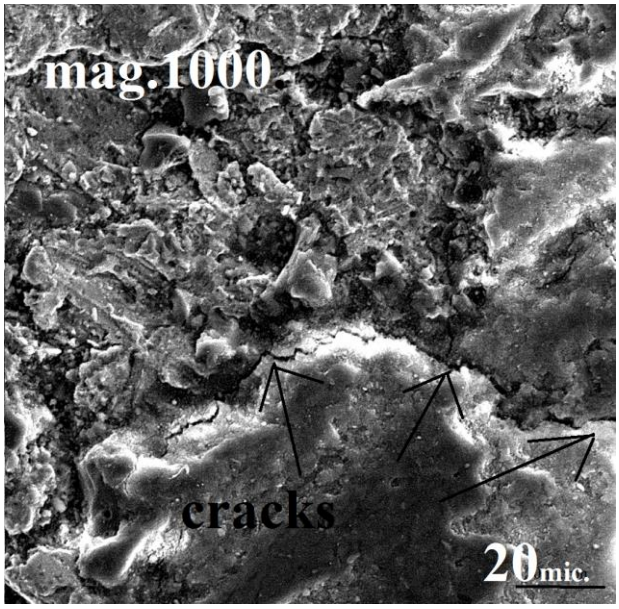

Fig. 13b. Cracks around the pin in G1A10 (x1000).

In the presented system, in addition to BAS, the nano alumina existences lead to lower TEC coating [15].

Therefore, by increasing the nano alumina content in composite, the residual stress arose from the TEC mismatch was excluded.

So, the residual stress becomes compressive in G1A15 that, the cracks caused by the pin effect, is omitted (unlike the cracks existence in the case of G1A5).

The incremental wear of almost all coatings decreases with sliding distance (with a exception of glass coatings) this is known to be due to the mirror surface effect, wear derbies, rolling effect and weight gain effect from materials transfer as the sliding distance increase. Generally wear resistance increases with decreasing wear rate [16,17].

4. CONCLUSION

The glass compositions $40SiO_2$-$20B_2O_3$-$17Na_2O$ (G1) suitable for application on steel alloys has been developed.

The coatings were successfully applied as a single coat by simple vitreous enameling process onto already prepared steel surfaces. The proposed coating material possesses a reasonable low melting (1250 ˚C) and processing 525-870 ˚C temperature, leading to less cost and energy consumption during preparation and application.

Sintering and crystallization of the enamel was investigated. Sodium silicate was the phase of mentioned glazes.

On the basis of the performed experiment, it was found out that with usage of nano alumina particles with the different weight content as the composites elements, enamel slurry shows higher surface tension and wetting angle (69º) compared to the slurry without alumina (< 44º), and therefore its rheological properties such as thixotropy are increased. It is necessary to consider this found experience during application of enamel slurry in practice. Furthermore, the high surface tension of nano alumina bearing slips can be considered as a restriction in enamels control.

The wear resistance of enamels reaches a plateau at low distances (50 m), which corresponds to the changeover from a glass matrix to an alumina matrix. The wear resistance of the alumina-matrix composite coatings is higher than the quartz containing coatings, which has been reported by others [3].

Acknowledgements

The author acknowledges the financial support of coating Project, Contract No. 93021874, from The Iran National Science Foundation (INSF).

REFERENCES

[1] N.N. Kruglitskii, A.S.M Makarov and V.F. Galinska, 'Control of rheological properties of enamel slips', *0361/7610/77/0910-0555507.50 9 1978 Plenum Publishing Corporation.*

[2] O. Ogle and N. Byles, 'Nanotechnology in Dentistry Today', *West Indian Med J*, vol. 63, no. 4, pp. 344–348, 2014.

[3] Y. Han, S.Y. Yao, W.W. Zhang, M. Gu and Y.S. Yao, 'A Novel Wear Resistant Glass Ceramic Coating materials', *Materials Science Forum,* vol. 686, pp. 521-527, 2011.

[4] M. Chen, W. Li, M. Shen, S. Zhu and F. Wang, 'Glass coatings on stainless steels for high-temperature oxidation protection: Mechanisms', *Corrosion Science*, vol. 82, pp. 316–327, 2014.

[5] A.H. Ataiwi, I.A. Mahmood and J.H. Mohmmed, 'Wear Resistance of a New Glass Ceramic coating', *Eng. &Tech. Journal*, vol. 32, no. 6, pp. 1472-1484, 2014.

[6] M.S. Belopol'skii, 'Rheological and casting properties of ceramic slips', *Science in the Ceramics Industry,* vol. 48, no. 3, pp. 120-125, 1991.

[7] R. Moreno, A. Salomoni and I. Stamenkovic, 'Influence of slip rheology on pressure casting of alumina', *Journal of the European Ceramic Society* , vol. 17, no. 2–3, pp. 327-331, 1997.

[8] J.H. Wu, M.S. Yen, C.W. Chen, M.C. Kuo, F.K. Tsai, J.S. Kuo, L.H. Yang and J.C. Huang, 'Isothermal crystallization behavior of nano-alumina particles-filled poly(ether ether ketone) composites', *journal of applied polymer science*, vol. 125, no. 1, pp. 494–504, 2012.

[9] J. Matej and A. Langrova 'Reaction products and corrosion of molybdenum electrode in glass melt containing antimony oxides and sodium sulfate', *Cer. Silikáty*, vol. 56, no. 3, pp. 280-285, 2012.

[10] K.K. Biswas, S. Datta, S.K. Das, M.C. Ghose, A. Mazumdar and N. Roy, 'Glass-ceramic Coatings for Steel and Nimonic Alloy', *Trans. Ind.Cer. Soc*., vol. 45, no. 2, pp. 43-45, 1986.

[11] B.S. Majumdar and G.M. Newaz, 'Constituent damage mechanisms in metal matrix composites under fatigue loading, and their effects on fatigue life', *Mat. Sci. and Eng. A*, vol. 200, no. 1-2, pp. 114-129, 1995.

[12] D.B. Dingwell, H.St.C. O'Neill, W. Ertel and B. Spettel, 'The solubility and oxidation state of nickel in silicate melt at low oxygen fugacities', *Geochimica et Cosmochimica Acta*, vol. 58, no. 8, pp. 1967-1974, 1994.

[13] N. Radhika and R. Raghu, 'Evaluation of Dry Sliding Wear Characteristics of LM 13 Al/B4C Composites', *Tribiology in Industry*, vol. 37, no. 1, pp. 20-28, 2015.

[14] L.A. Gorelova et al., 'Thermal expansion and structural complexity of Ba silicates with tetrahedrally coordinated Si atoms', *J. Sol. St. Chem.*, vol. 235, pp. 76-84, 2016.

[15] S. Arcaro, M.I. Nieto, R. Moreno and A.P. Novaes de Oliveira, 'The influence of nano alumina additions on the coefficient of thermal expansion of a LZS glass–ceramic composition', *Ceramic International,* vol. 42, no. 7, pp. 8620–8626, 2016.

[16] M.A. Chowdhury and D.M. Nuruzzaman, 'Experimental Investigation on Friction and Wear Properties of Different Steel Materials', *Tribology in Industry*, vol. 35, no. 1, pp. 42-50, 2013.

[17] L. Capitanu, J. Onisoru and A. Iarovici, 'Tribological aspects for injection processing of thermoplastic composite materials with glass fiber', *Tribology in Industry,* vol. 26, No. 1&2, pp. 32-41, 2004.